The NASA-JAXA Global Precipitation Measurement mission – part I: New frontiers in precipitation

The NASA-JAXA Global Precipitation Measurement mission – part I: New frontiers in precipitation

Daniel Watters[1,2] and **Alessandro Battaglia**[1,2,3]

[1]*Earth Observation Science Group, Department of Physics and Astronomy, University of Leicester, UK*
[2]*National Centre for Earth Observation, University of Leicester, UK*
[3]*DIATI, Politecnico di Torino, Italy*

The need for global measurement of precipitation

Precipitation is a key component of the water cycle. Its formation involves different phases of water across the whole troposphere down to the Earth's surface, with the latent heat release of each phase transition strongly affecting the atmospheric energy budget. Precipitation is paramount to society, for example, by providing a source of freshwater and supporting agriculture. However, precipitation (or the lack of) can also be destructive: Droughts can result in food and water shortages, while severe storms can cause flooding and structural damage. As such, the meteorological community strives to understand, quantify and predict precipitation across the globe.

Observations are vital to characterising global precipitation and providing a reference for current weather (short-term) and climate (long-term) prediction models. However, measuring precipitation across the entire globe is difficult from a ground-based perspective. Ground-based precipitation gauges, which arguably provide the most direct measurements since they capture precipitation, only cover an area equal to approximately less than half of a football pitch (Kidd *et al.*, 2017) and are scarce over the oceans and sparsely populated regions (excluding the USA and Australia; see figure 1 of Kidd and Huffman, 2011). Ground-based radar networks, which indirectly estimate precipitation by transmitting electromagnetic radiation into the atmosphere and measuring the radiation backscattered from precipitation, provide observations limited to some land regions (the USA, Europe, China, South Africa, India, etc.), islands (Maritime Continent, New Zealand, Japan, etc.), and coastlines (Australia, east coast of South America; see figure 1 of Saltikoff *et al.*, 2019).

Measuring global precipitation from space

From a spaceborne perspective, measuring global precipitation becomes more accessible, thanks to satellites orbiting around the Earth, which can observe even remote areas of the planet. However, spaceborne sensors use remote sensing techniques and therefore only provide indirect measurements of precipitation. There are two types of sensors: passive sensors, which measure the radiation naturally emitted and/or scattered from the earth-atmosphere system in the direction of the sensor, and active sensors, which send pulses of radiation and measure its backscatter in the direction of the sensor. Microwave frequencies/wavelengths in the range 10–200GHz (1.5mm to 3cm) are typically selected for measuring precipitation with spaceborne passive and active sensors, as there is little absorption of the radiation by atmospheric gases at most frequency bands. However, there are several microwave bands at which atmospheric gases are strongly absorbing (water vapour at ~22GHz and ~183GHz, oxygen at ~60GHz and ~118GHz; see figure A1 of Battaglia *et al.*, 2020). These bands are typically avoided by passive microwave imagers and active sensors, and exploited by passive microwave sounders. Furthermore, for active precipitation sensors (i.e. radars), usable microwave wavelengths are constrained by: the antenna size and power of the radar, wavelengths that are free of military and civilian use, and wavelengths that are long enough to penetrate through clouds without substantial attenuation (i.e. loss of radiation due to scattering and/or absorption). Longer-wavelength/lower-frequency radars (>3cm/<10GHz) typically require more power, greater finance and larger antennas (to retain a small beamwidth) that are not favourable for operations on-board satellites (Rauber and Nesbitt, 2018). Hence, spaceborne radar frequencies/wavelengths of 13.6GHz (2.2cm) and 35.5GHz (8.5mm) are typically selected for sensing precipitation and 94GHz (3.2mm) for sensing clouds and

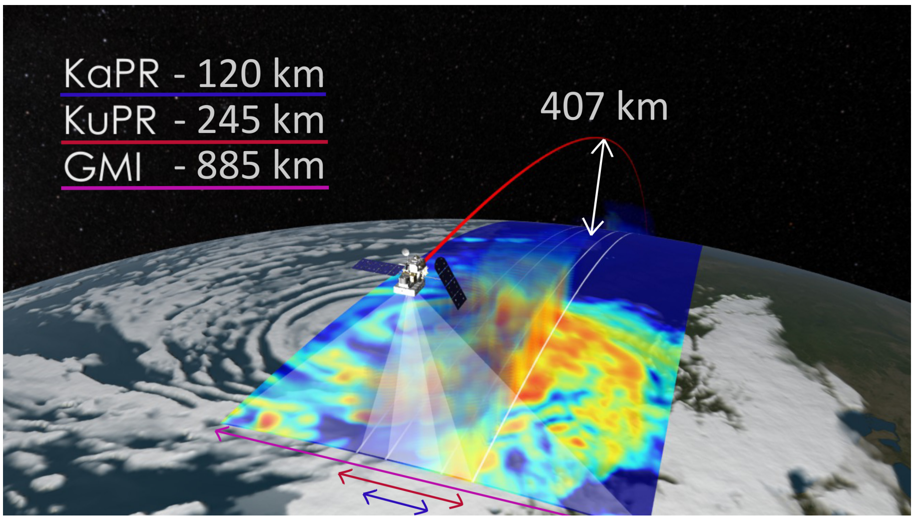

Figure 1. The GPM-CO measuring over a mid-latitude storm. The red, white, magenta, maroon and blue lines indicate the flight path, satellite altitude, GMI swath, DPR Ku-band (or KuPR) swath and DPR Ka-band (or KaPR) swath, respectively. The three-dimensional rainfall is heaviest where red and lightest where dark blue; note how three-dimensional measurements are only available from the DPR segment of the swath. The Ka-band swath was extended to 245km to match the Ku-band swath on 21 May 2018; refer to Iguchi (2020) for more details. (Credit: NASA Goddard Space Flight Center Scientific Visualization Studio; adapted from original image.)

Weather – 00 2020, Vol. 00, No.

light precipitation; they are of the order of the size of precipitation particles such that the particles will scatter a significant fraction of the incident radiation back towards the sensor.

Spaceborne passive sensors are more limited in measuring precipitation than active sensors since passive sensors do not have ranging capabilities (i.e. the capability to determine the range from the sensor to precipitation particles). Active sensors calculate the range by measuring the time between pulse transmission and reception of the radiation backscattered at the sensor. Without ranging capabilities, passive microwave sensors measure intensities of radiation (or brightness temperatures after conversion via the Planck Function) that are an integral of a complex function over the whole vertical column; this function includes the temperature and emissivity of the surface, as well as the temperature, absorption/emissivity and scattering properties of precipitation, clouds and the atmospheric gases (e.g. the water vapour component at microwave frequencies). Passive microwave sounders measure in and around the water vapour and oxygen absorption bands, to sound atmospheric humidity and temperature, respectively. Conversely, passive microwave imagers measure outside of the absorption bands where the surface (and clouds/precipitation) generally provides a dominant contribution. Identifying precipitation with imagers differs between land and ocean. Over ocean, precipitation generally produces an increase in brightness temperature due to the emission by precipitation against the radiometrically cold, low emissivity ocean background (e.g. see figure 2f of Watters *et al*., 2018). Identification of precipitation over land is more difficult due to its higher surface emissivity compared to the ocean; the surface emissivity is higher so any relative change in brightness temperature due the precipitation's emission is much smaller, even in cases where the precipitation is strongly absorbing and emitting (i.e. optically thick). However, precipitation can be identified over land by the scattering of microwave radiation that can cause a significant reduction in the brightness temperature; rain has a low scattering efficiency while ice has a higher scattering efficiency, so reductions in brightness temperature are more easily identified in precipitating columns containing ice. Brightness temperature reductions due to scattering are not usually found over the ocean due to its low emissivity, though they have been identified in severe hailstorms (e.g. see figure 9 of Marra *et al*., 2017).

From a spaceborne perspective, active radars are better suited to measuring precipitation than passive microwave radiometers as they provide ranging capabilities that allow for precipitation profiling and they have smaller measurement footprints that better capture the high spatial variability of precipitation. While radar provides better measurements of precipitation, it lacks the spatial coverage of radiometers; only one precipitation radar is currently in space (compared to about 10 passive microwave radiometers) and it has a smaller swath. Unlike gauges, precipitation radar does not directly measure precipitation. Instead, radar measures the fraction of the radar-transmitted electromagnetic signal that is backscattered to the radar from the target, from which the radar reflectivity factor is calculated. The challenge is in the conversion from the radar reflectivity factor to precipitation rate. This conversion depends upon the distribution and composition (microphysics) of precipitation particles within the atmospheric backscattering volume, as well as the attenuation of the electromagnetic pulse as it travels to and from the precipitation volume.

The Global Precipitation Measurement mission's Core Observatory

The Global Precipitation Measurement (GPM) mission's Core Observatory (CO), jointly operated by the National Aeronautics and Space Administration (NASA) and the Japanese Aerospace Exploration Agency (JAXA), was launched in February 2014 (Hou *et al*., 2014; Skofronick-Jackson *et al*., 2017, 2018; Kidd *et al*., 2020). The satellite is the successor to NASA and JAXA's first precipitation-measuring satellite, the Tropical Rainfall Measuring Mission (TRMM; Simpson *et al*., 1996; Kummerow *et al*., 1998), which provided a 17-year record of tropical and subtropical precipitation. The GPM-CO flies in a low-Earth non-Sun-synchronous orbit like TRMM, but with a greater inclination of 65° (35° for TRMM) to provide measurements over the mid-latitudes as well as the tropics and subtropics (Figure 1).

The Dual-frequency Precipitation Radar (DPR) on-board the GPM-CO is only the second radar to measure precipitation from space, after the Precipitation Radar (PR) on TRMM (Iguchi *et al*., 2018; Iguchi, 2020). The GPM DPR improves upon the preceding TRMM PR by providing measurements of precipitation at two frequencies: the previously selected Ku-band (13.6GHz), and (the new) Ka-band (35.5GHz). The Ku-band has a detection threshold of ~0.32mmh^{-1} (15dBZ), while the Ka-band has a detection threshold of ~0.27–0.56mmh^{-1} (14–19dBZ; Iguchi, 2020). The addition of the Ka-band frequency aims at improving the accuracy of estimating precipitation rate, at better identifying the height at which precipitation changes phase, and at characterising the precipitation drop size distribution (Iguchi *et al*., 2018). The strength of these spaceborne precipitation radars is their ability to provide three-dimensional measurements of precipitation systems (Battaglia *et al*., 2020); the GPM DPR has a vertical resolution of 0.25km and horizontal resolution of 5km (Hou *et al*., 2014). The introduction of GPM DPR mid-latitude measurements has enabled the ability to capture the three-dimensional structure of extratropical cyclones and snowfall events for the first time, while the multi-frequency capability over the tropics has resulted in improved measurements for better understanding of the structure of tropical cyclones (hurricanes, typhoons). The second instrument on-board the GPM-CO, the GPM Microwave Imager (GMI), also supersedes its TRMM counterpart (the TRMM Microwave Imager, TMI) with the inclusion of four extra channels. The 166GHz vertical and horizontal polarisation (V & H) channels are used for detecting light precipitation beyond the tropics, and the 183.31 ± 3GHz and 183.31 ± 7GHzV channels are used for detecting light snow and rain over snowy land and ice clouds with smaller ice particles (Hou *et al*., 2014; Rysman *et al*., 2019).

The Global Precipitation Measurement mission's satellite constellation

GPM's primary goals include improving spaceborne observations of precipitation and advancing our understanding of precipitation systems (Skofronick-Jackson *et al*., 2017, 2018). The GPM satellite constellation addresses these goals at the global scale. The constellation is formed of several satellites from international space agencies, with satellite systems continuously evolving over time (Figure 2). The passive microwave radiometers on-board all constellation satellites, each travelling in a different non-Sun-synchronous or polar orbit, are intercalibrated by the GPM-CO GMI (Berg *et al*., 2016). The GPM constellation is a key contributor to NASA's global-gridded precipitation product, otherwise known as the Integrated Multi-satellitE Retrievals for GPM (IMERG) product (Huffman *et al*., 2019, 2020). The current IMERG version-6 product now incorporates TRMM measurements (June 2000 to May 2014) as well as GPM measurements (June 2014 to present).

The IMERG algorithm is outlined as follows (Huffman *et al*., 2019, 2020). Intercalibrated brightness temperatures from the majority of the GPM/TRMM constellation of microwave radiometers are converted into precipitation estimates using the Goddard Profiling algorithm (Kummerow *et al*., 2015). The single exception is the Sounder for Probing Vertical Profiles of Humidity (SAPHIR) on-board Megha-Tropiques from which pre-

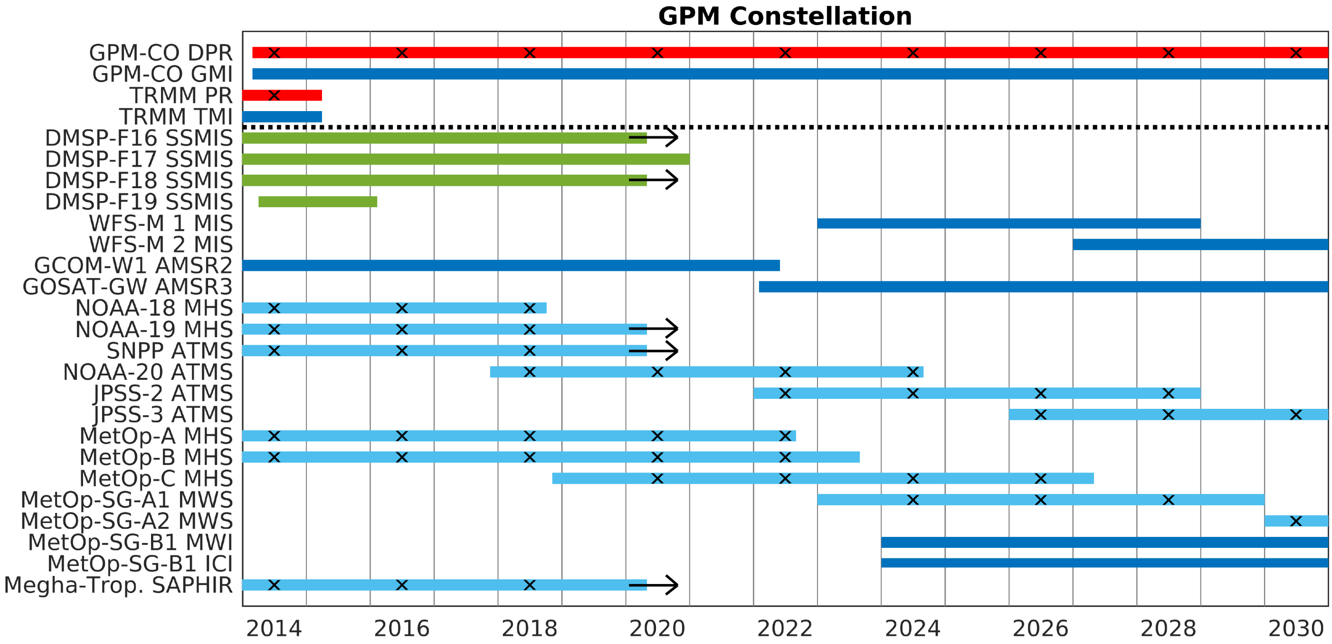

Figure 2. A timeline of the GPM constellation of spaceborne radars and passive microwave radiometers. The constellation consists of sensors on-board: the NASA-JAXA GPM-CO and TRMM; the National Oceanic and Atmospheric Administration (NOAA) and the US Department of Defense's (DoD) Defense Meteorological Satellite Program (DMSP) Block 5D-3 series; the US DoD's Weather System Follow-on Microwave (WSF-M) satellites; JAXA's Global Change Observation Mission for Water 1 (GCOM-W1); JAXA and the Japan Ministry of the Environment's (MOE) Global Observation SATellite for Greenhouse gases and Water cycle (GOSAT-3/GW); NOAA's Satellite 18 and 19 (NOAA-18, -19); NOAA and NASA's Joint Polar Satellite Series (NOAA-20, Suomi National Polar-orbiting Partnership/SNPP, JPSS-2, -3); the European Organisation for the Exploitation of Meteorological Satellites (EUMETSAT) and the European Space Agency's (ESA) Meteorological Operational Satellite (MetOp) EUMETSAT Polar System First Generation (Met-Op-A, -B, -C) and Second Generation (MetOp-SG-A1, -A2, -B1); the Indian Space Research Organisation (ISRO) and the Centre National d'Etudes Spatiales' (CNES) Megha-Tropiques. The colour of the timeline bar indicates the type of sensor (red for radar, dark blue for passive microwave imager, light blue for passive microwave sounder, and green for passive microwave imager and sounder), and crosses along the bar indicate a cross-track scan (those without crosses perform conical scans). Arrows at the end of bars indicate that the satellite's lifetime expectancy has been exceeded with no end-of-life date determined. Sensor information available from OSCAR (2020) and Huffman et al. (2019).

cipitation estimates are produced using the Precipitation Retrieval and Profiling Scheme (Kidd, 2018). The IMERG algorithm then grids and calibrates these microwave precipitation estimates to the Combined Radar-Radiometer product (CORRA; Olson *et al.*, 2016; Grecu and Olson, 2020); CORRA estimates are determined from TRMM PR-TMI or GPM-CO DPR-GMI measurements, dependent on the era. Beforehand, CORRA is calibrated at the zonal average scale to the satellite-gauge Global Precipitation Climatology Project's version-2.3 product (Adler *et al.*, 2003; 2018) over high-latitude oceans (where CORRA is biased low) and over tropical land (where CORRA is biased high). Calibration of the microwave precipitation estimates to CORRA is a two-step process: first, TRMM/GPM constellation estimates are calibrated to TMI/GMI estimates, then TMI/GMI estimates are calibrated to CORRA (and this calibration is applied to the TMI/GMI-calibrated constellation estimates). These CORRA-calibrated snapshot estimates are then propagated by motion vectors of total column water vapour (Tan *et al.*, 2019) and subject to quasi-Lagrangian time interpolation (known as morphing; Joyce *et al.*, 2004) in order to increase the global coverage of the precipitation estimates. Motion vectors are derived from the Modern-Era Retrospective Analysis for Research and Applications (MERRA-2) reanalysis product in the Final Run of IMERG (research-level product; 3.5 months latency), and from the Goddard Earth Observing System Forward Processing model product in the Early and Late Run (near-real-time products; 4h and 12h latency, respectively) (Tan *et al.*, 2019). Infrared precipitation estimates (Hong *et al.*, 2004), which are calibrated to the microwave estimates, fill in the remaining coverage gaps between 60°N-S. In the Final Run, IMERG half-hour estimates are calibrated by gauge estimates from the Deutscher Wetterdienst Global Precipitation Climatology Centre Full/Monitoring product (Schneider *et al.*, 2014) over land. IMERG Early and Late Run products are not currently climatologically calibrated to the Final Run product. The product currently provides a 20-year record (June 2000 to present) of precipitation estimates across both the TRMM and GPM eras at 0.1° and half-hour resolution, with full coverage in the 60° N-S region and partial coverage elsewhere (over snow/ice-free surfaces).

Conclusion

This article outlines how the spaceborne NASA-JAXA GPM mission addresses the challenge of global measurement of precipitation. The rationale underpinning the mission is described from first principles, including the greater access and coverage that a spaceborne perspective provides, and the remote sensing techniques and instrumentation required to measure precipitation from space. Advantages and limitations of the passive and active microwave sensors are discussed, and the details of such instruments on-board the GPM-CO and constellation of international satellites are provided.

New frontiers in precipitation science from the GPM mission are highlighted. The GPM mission provides the most advanced precipitation and latent heat estimates from space, surpassing those from its predecessor mission, TRMM. In particular, GPM extends the tropical and subtropical coverage of TRMM into the mid-latitudes, and adds a second frequency (Ka-band, 8.5mm) to its radar and four further channels to its microwave radiometer.

The GPM mission lays the foundation of a new approach to measuring precipitation with global coverage and short revisit time enabled by a constellation of passive microwave radiometers calibrated by the GPM-CO sensors. This microwave constellation underpins the IMERG product, which combines measurements from the GPM microwave constellation, infrared sensors and ground-based gauges, providing precipitation estimates at 0.1° spatial resolution and half-hourly temporal resolution. In mid-2019, NASA extended the period of IMERG estimates back from 2014 to 2000 to include not only the GPM constellation measurements but also the TRMM era. The dataset is currently available from June 2000 (with plans to go back to 1998), providing a 20-year-plus climatological record of precipitation observations.

Part II of this article (Watters and Battaglia, 2020) applies GPM precipitation estimates to two applications: the case study of Hurricane Irma and a 20-year precipitation climatology. Precipitation estimates from the GPM-CO sensors are used to analyse a snapshot of the three-dimensional structure of Hurricane Irma, and the IMERG product is used to determine the evolution of surface precipitation along the hurricane track. Latent heat estimates, derived from reflectivity profiles and precipitation estimates from the GPM-CO sensors, are used to describe the energetics of the hurricane. Also, the 20-year IMERG precipitation climatology is compared to other precipitation climatologies, with differences discussed.

Acknowledgements

Daniel Watters was funded by a Natural Environment Research Council studentship awarded through the Central England NERC Training Alliance (CENTA; grant reference NE/L002493/1) and by the University of Leicester. The work by Alessandro Battaglia was supported by the project 'Radiation and Rainfall' funded by the UK National Centre for Earth Observation (Contract RP18G0002). This research used the SPECTRE High Performance Computing Facility at the University of Leicester. The authors thank an anonymous reviewer and Edward Graham for their helpful comments and recommendations that greatly helped to improve the manuscript.

References

Adler RF, **Huffman GJ**, **Chang A** ***et al***. 2003. The version-2 Global Precipitation Climatology Project (GPCP) monthly precipitation analysis (1979-present). *J. Hydrometeorol.* **4**(6): 1147–1167.

Adler RF, **Sapiano MR**, **Huffman GJ** ***et al***. 2018. The Global Precipitation Climatology Project (GPCP) monthly analysis (new version 2.3) and a review of 2017 global precipitation. *Atmos.* **9**(4): 138.

Battaglia A, **Kollias P**, **Dhillon R** ***et al***. 2020. Space-borne cloud and precipitation radars: status, challenges and ways forward. *Rev. Geophys.* **58**(3): e2019RG000686. doi: 10.1029/2019RG000686

Berg W, **Bilanow S**, **Chen R** ***et al***. 2016. Intercalibration of the GPM microwave radiometer constellation. *J. Atmos. Oceanic Tech.* **33**(12): 2639–2654.

Grecu M, **Olson WS**. 2020. Precipitation retrievals from satellite combined radar and radiometer observations, in *Satellite Precipitation Measurement*. Springer: Cham, Switzerland, pp 231–248.

Hong Y, **Hsu KL**, **Sorooshian S** ***et al***. 2004. Precipitation estimation from remotely sensed imagery using an artificial neural network cloud classification system. *J. Appl. Meteorol.* **43**(12): 1834–1853.

Hou AY, **Kakar RK**, **Neeck S** ***et al***. 2014. The global precipitation measurement mission. *Bull. Am. Meteorol. Soc.* **95**(5): 701–722.

Huffman GJ, **Bolvin DT**, **Braithwaite D** ***et al***. 2019. NASA Global Precipitation Measurement (GPM) Integrated Multi-satellitE Retrievals for GPM (IMERG). Algorithm theoretical basis document, version 6, NASA, 38 pp. https://pmm.nasa.gov/sites/default/files/document_files/IMERG_ATBD_V06.pdf (accessed 8 July 2020).

Huffman GJ, **Bolvin DT**, **Braithwaite D** ***et al***. 2020. Integrated multi-satellite retrievals for the Global Precipitation Measurement (GPM) mission (IMERG), in *Satellite precipitation measurement*. Springer: Cham, Switzerland, pp 343–353.

Iguchi T. 2020. Dual-frequency Precipitation Rradar (DPR) on the Global Precipitation Measurement (GPM) mission's Core Observatory, in *Satellite Precipitation Measurement*. Springer: Cham, Switzerland, pp 183–192.

Iguchi T, **Seto S**, **Meneghini R** ***et al***. 2018. GPM/DPR level-2. Algorithm theoretical basis document, version 6, JAXA, 127 pp. https://www.eorc.jaxa.jp/GPM/doc/algorithm/ATBD_DPR_201811_with_Appendix3b.pdf (accessed 3 February 2020).

Joyce RJ, **Janowiak JE**, **Arkin PA** ***et al***. 2004. CMORPH: a method that produces global precipitation estimates from passive microwave and infrared data at high spatial and temporal resolution. *J. Hydrometeorol.* **5**(3): 487–503.

Kidd C. 2018. NASA Global Precipitation Measurement (GPM) Precipitation Retrieval and Profiling Scheme (PRPS). Algorithm theoretical basis document, version 01-02, NASA, 17 pp. https://pps.gsfc.nasa.gov/Documents/20180203_SAPHIR-ATBD.pdf (accessed 7 July 2020).

Kidd C, **Huffman G**. 2011. Global precipitation measurement. *Meteorol. Appl.* **18**(3): 334–353.

Kidd C, **Becker A**, **Huffman GJ** ***et al***. 2017. So, how much of the earth's surface is covered by rain gauges? *Bull. Am. Meteorol. Soc.* **98**(1): 69–78.

Kidd C, **Takayabu YN**, **Skofronick-Jackson GM** ***et al***. 2020. The Global Precipitation Measurement (GPM) mission, in *Satellite Precipitation Measurement*. Springer: Cham, Switzerland, pp 3–23.

Kummerow C, **Barnes W**, **Kozu T** ***et al***. 1998. The Tropical Rainfall Measuring Mission (TRMM) sensor package. *J. Atmos. Oceanic Tech.* **15**(3): 809–817.

Kummerow CD, **Randel DL**, **Kulie M** ***et al***. 2015. The evolution of the Goddard profiling algorithm to a fully parametric scheme. *J. Atmos. Oceanic Tech.* **32**(12): 2265–2280.

Marra AC, **Porcù F**, **Baldini L** ***et al***. 2017. Observational analysis of an exceptionally intense hailstorm over the Mediterranean area: role of the GPM Core Observatory. *Atmos. Res.* **192**: 72–90.

Olson WS, **Masunaga H**, GPM Combined Radar-Radiometer Algorithm Team. 2016. GPM Combined Radar-Radiometer Precipitation. Algorithm theoretical basis document, version 4, NASA, 63 pp. https://gpm.nasa.gov/sites/default/files/document_files/Combined_algorithm_ATBD.V04.rev_.pdf (accessed 19 February 2020).

OSCAR. 2020. World Meteorological Organization's observing systems capability analysis and review tool. https://www.wmo-sat.info/oscar/spacecapabilities (accessed 17 May 2020).

Rauber RM, **Nesbitt SW**. 2018. *Radar Meteorology: A First Course*. John Wiley & Sons: Hoboken, NJ.

Rysman J-F, **Panegrossi G**, **Sanò P** ***et al***. 2019. Retrieving surface snowfall with the GPM Microwave Imager: a new module for the SLALOM algorithm. *Geophys. Res. Lett.* **46**(22): 13593–13601.

Saltikoff E, **Friedrich K**, **Soderholm J** ***et al***. 2019. An overview of using weather radar for climatological studies: successes, challenges, and potential. *Bull. Am. Meteorol. Soc.* **100**(9): 1739–1752.

Schneider U, **Becker A**, **Finger P** ***et al***. 2014. GPCC's new land surface precipitation climatology based on quality-controlled in situ data and its role in quantifying the global water cycle. *Theor. Appl. Climatol.* **115**(1–2): 15–40.

Simpson J, **Kummerow C**, **Tao W-K** ***et al***. 1996. On the Tropical Rainfall Measuring Mission (TRMM). *Meteorol. Atmos. Phys.* **60**(1–3): 19–36.

Skofronick-Jackson G, **Petersen WA**, **Berg W** ***et al***. 2017. The Global Precipitation Measurement (GPM) mission for science and society. *Bull. Am. Meteorol. Soc.* **98**(8): 1679–1695.

Skofronick-Jackson G, **Kirschbaum D**, **Petersen W** ***et al***. 2018. The Global Precipitation Measurement (GPM) mission's scientific achievements and societal contributions: reviewing four years of advanced rain and snow observations. *Q. J. R. Meteorol. Soc.* **144**(S1): 27–48.

Tan J, **Huffman GJ**, **Bolvin DT** ***et al***. 2019. IMERG V06: changes to the morphing algorithm. *J. Atmos. Oceanic Tech.* **36**(12): 2471–2482.

Watters D, **Battaglia A**. 2020. The NASA-JAXA global precipitation measurement mission: new frontiers in precipitation science – part II. *Weather*. doi: 10.1002/wea.3869.

Watters D, **Battaglia A**, **Mroz K** ***et al***. 2018. Validation of the GPM version-5 surface rainfall products over Great Britain and Ireland. *J. Hydrometeorol.* **19**(10): 1617–1636.

Correspondence to: D. Watters

dcw17@leicester.ac.uk

doi: 10.1002/wea.3865